

Signal Conditioning for Sophisticated Transducers

A substantial amount of information is available on signal conditioning for common transducers. Fortunately, most of these devices, which are used to sense common physical parameters, are relatively easy to signal condition. Further, most transducer-based measurement requirements are well served by standard transducers and signal conditioning techniques.

Some situations, however, require sophisticated transduction techniques with their attendant special signal conditioning requirements. This application note details signal conditioning and applications information for a diverse group of sophisticated and unusual transducers. Because these devices are unusual or somewhat difficult to signal condition, relatively little material has appeared on how to design circuitry for them. Many of these devices permit measurements which cannot be accomplished in any other way. For this reason it is worthwhile to have a basic familiarity with

National Semiconductor
Application Note 301



their capabilities and what is required to signal condition them. The circuits shown are intended as instructive examples only, although each one has been constructed and tested. Every individual transducer application has a set of specifications and constraints which will require modification or revision of the circuits presented. Sources of additional information which feature more vigorous treatment are presented in a reference section at the end of the application note.

PHOTOMULTIPLIER TUBE (PMT)

Perhaps the most versatile light detector available is the photomultiplier tube (PMT). These sensors allow single photon detection, sub-nanosecond rise time, bandwidths approaching 1 GHz and linearity of response over a range of 10^7 . In addition, they feature extremely low noise, stable characteristics and very long life. *Figure 1a* details a typical

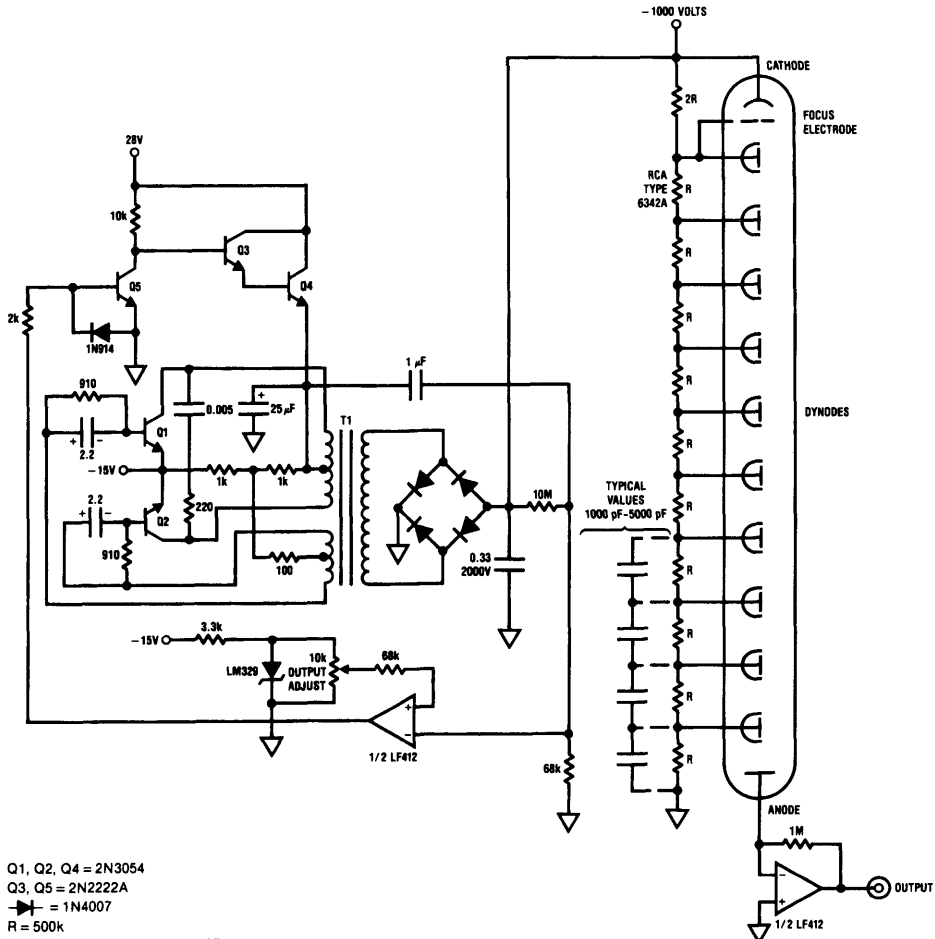


FIGURE 1a

TL/H/5641-1

PMT along with a signal conditioning circuit. The tube is composed of a photosensitive cathode, an anode, a focusing electrode and ten dynode stages. In operation, the photocathode, which is high voltage biased with respect to the dynodes, emits photoelectrons when it is struck by light. These are focused into a beam and directed to the first dynode stage by the focus electrode. These arriving electrons impinge on the dynode, causing secondary emission to occur. As a result, a greater number of electrons leave the dynode and are then directed to the second dynode. In this fashion, a number (e.g., 10) of dynode stages are used to achieve overall gains of 10^6 to 10^8 . The electrons from the final dynode are collected by the anode, which provides the output current of the tube. In contrast to other vacuum tubes, the PMT does not use a filament to thermionically generate electrons. Instead, the photocathode, in combination with incident light, initiates the electrons. The absence of a filament means there are no degradation, heat or out-gassing problems and the life of a PMT is very long.

Signal conditioning involves generating a stable high voltage supply and accomplishing a low noise current-to-voltage conversion at the anode. In this example, a DC-DC converter is used to supply the dynode potentials to the tube. The supply is stabilized by the LF412 amplifier which drives the Q3-Q5 combination to complete a feedback loop around the Q1-Q2 driven transformer. The LM329 provides a stable servo reference. In general, the regulation of a PMT supply should be at least ten times greater than the required measurement gain stability because of the relationship between a PMT's gain slope and the high voltage applied. The cathode and dynodes are biased from the high voltage supply via divider resistors. The resistors distribute the dynode potentials in proportion to a ratio which is specified for each tube type. To prevent non-linear response, the current through the divider string should be at least ten times the maximum expected current out of the tube. Some high speed pulse applications can generate transient high tube currents which may require the small capacitors shown in dashed lines. The anode is the tube output and appears as an almost ideal current source. The LF412 amplifier performs a current-to-voltage conversion with the 1 M Ω resistor setting the output scale factor.

The PMT's combination of high speed and extreme sensitivity suits it to a variety of difficult light measurement chores. The remarkable photograph of *Figure 1b* shows the actual rise and fall time characteristics (inverted) of a fast pulse of

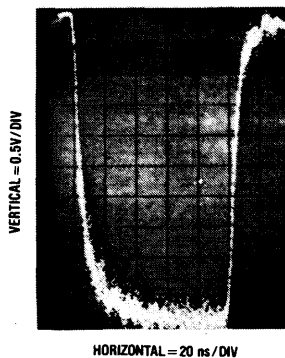


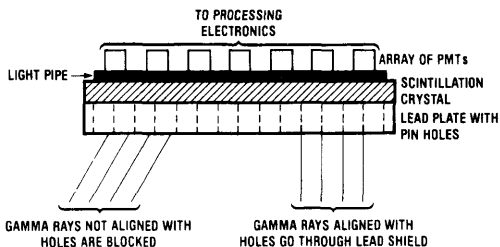
FIGURE 1b

TL/H/5641-2

light produced by an LED. This photo was taken with a high speed PMT which was terminated directly into a 1 GHz bandwidth, 50 Ω sampling oscilloscope.

Another PMT application exchanges speed for sensitivity in a nuclear medical instrument, the Gamma camera.

The Gamma camera operates by using the scintillation properties of special crystals which are placed in front of an array of PMTs. Small quantities of radioactive isotopes are introduced into the patient either by oral ingestion or injection. Specific isotopes collect at certain organs within the body. As the radioactive isotopes decay, gamma rays are emitted from the isotope concentration area. These rays are collimated by a lead plate containing many small holes which forms the front of the camera (*Figure 2a*). This collimator allows only those rays which are at right angles to pass through the plate. The rest are absorbed in the lead. In this fashion the geometric shape of the gamma source is preserved and is presented to the scintillation crystal. The array of PMTs is located behind the crystal. The individual tubes respond to any given scintillation anywhere in the crystal with a distribution of signal strengths. This distribution is used by a processor to determine the precise point of scintillation in the crystal. Each of these scintillation locations is recorded on a CRT. After a length of time, this counting-integration process produces a picture of the organ on the CRT. *Figure 2b* shows 7 such pictures of a pair of human lungs, taken 30 seconds apart over a 150 second period. In photo A, the administered radioactive isotope begins to collect in the lungs. In photo B, the lungs are saturated. During photos C, D, E, F and G, the isotope progressively decays. Normally, human lungs will clear after 120 seconds. This particular sequence shows evidence of an obstructive pulmonary disease which is most pronounced in the lower right lung.



TL/H/5641-3

FIGURE 2a

PYROELECTRIC DETECTOR

The pyroelectric detector represents another class of sophisticated photodetector. These ceramic-based radiation detectors feature an extraordinary light sensitivity range from microwatts to watts with excellent linearity. Their bandwidth is flat from the ultraviolet to the far infrared. Response is sub-nanosecond and the devices may be operated at room temperature; no cooling is required. A major difficulty and source of confusion with signal conditioning pyroelectrics is that they do not respond at DC. This limitation, which is in keeping with all ceramic-based transducers, is surmounted by using a light chopper in front of the detector. In this fashion, DC light inputs to the detector appear as a modulated carrier. These devices are used in industrial temperature measurement, spectroscopy and laser power meters. They are also used to measure high speed laser pulse characteristics.

For signal conditioning purposes, pyroelectrics can be modeled as either a current source with parallel capacitance or a voltage source with series capacitance. Because there is no resistive component, there is no resistive Johnson noise. *Figure 3a* shows a simple voltage mode set-up which can be used for fast pulses of high energy. In this circuit, the detector is terminated directly into a high speed 50Ω oscilloscope. In *Figure 3b*, a slower detector terminates into 1 MΩ and is unloaded by the LH0052 low bias FET amplifier. For

response time much longer than a few milliseconds, the optical chopper provides a modulated light signal to the detector. The amplifier output may be rectified to recover the DC component of the signal. *Figure 3c* shows a current mode signal conditioning circuit. The optical chopper is retained, but the detector is loaded directly into the summing junction of a low bias op amp composed of an LF411 and a pair of sub-picoamp bias FETs. The low bias current allows low energy light measurement.

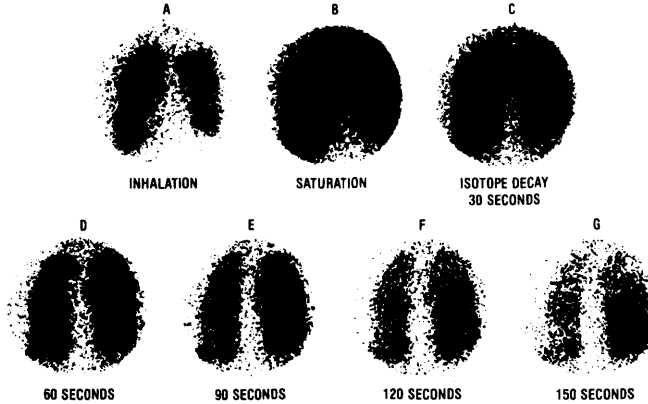


FIGURE 2b

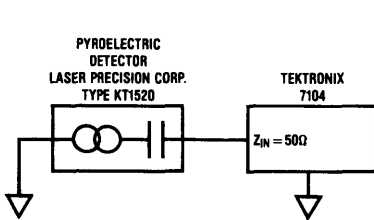


FIGURE 3a

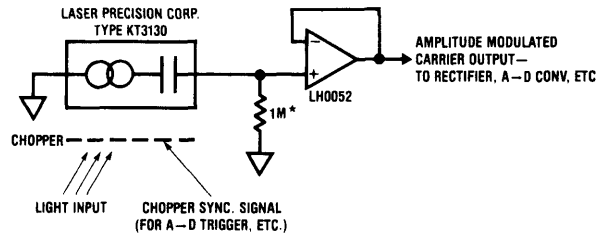
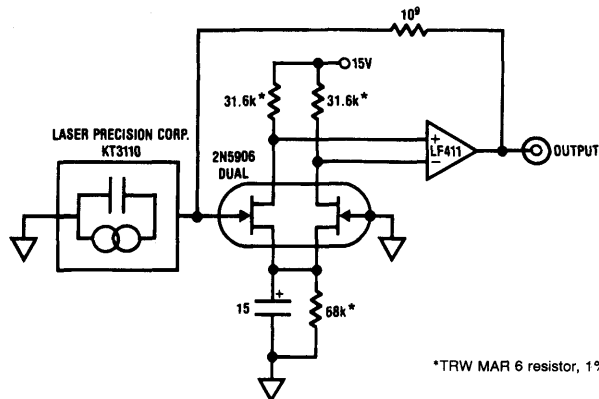


FIGURE 3b

*TRW MAR 6 resistor, 1%



*TRW MAR 6 resistor, 1%

FIGURE 3c

TL/H/5641-4

PIEZOELECTRIC ULTRASONIC RESONATORS

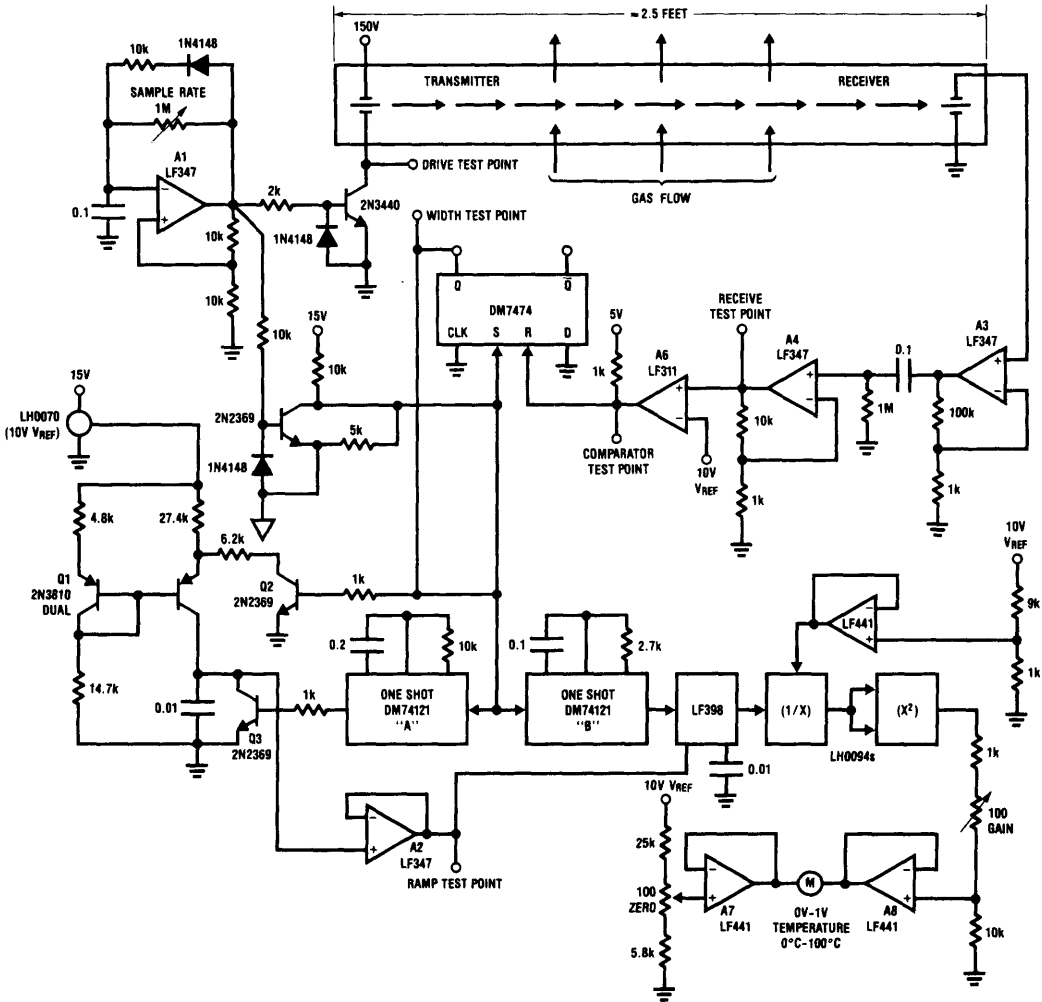
Piezoelectric ultrasonic transducers are generically related to pyroelectrics in that they are also ceramic-based. These devices are used for both generation and reception of narrow band ultrasonic information. The characteristic resonance of these transducers, in a similar fashion to quartz crystals, is extremely narrow, allowing high Q, noise rejecting systems to be built around them. As transmitters, they are often driven very hard by steps several hundred volts high at low duty cycles. This permits substantial ultrasonic power to be generated and eases the burden of the receiver in the system (which could be the same transducer as the transmitter). Ultrasonic resonators are used in a wide variety of applications including liquid level detection, intrusion alarms, automatic camera focusing, cardiac ultrasonic profiling (echocardiography) and distance measuring equipment. Figure 4a shows a signal conditioning circuit which capitalizes on the

high Q, noise rejection characteristics and fast response of ultrasonic transducers to accomplish a difficult thermal measurement. This circuit is similar to a type developed to measure high speed temperature shifts in a gas medium.

In contrast to almost all other temperature sensors, it does not rely on its sensing element to come into thermal equality with the measurand. Instead, the relationship between the speed of sound and the temperature of the medium in which the sound is propagating is utilized to determine temperature. The speed of response is therefore very fast and the measurement is also non-invasive. The relationship between the speed of sound in any medium and temperature may be described by equations. As an example, the relationship in dry air is:

$$C = 331.5 \sqrt{\frac{T}{273}} \text{ meters/second,}$$

where C = speed of sound.



Ultrasonic transducers = Massa MK-109

FIGURE 4a

TL/H/5641-5

For any given value of C the absolute temperature is:

$$T = \frac{273}{(331.5)^2} \times C^2.$$

It is clear that because sound speed and the medium in which it travels have a predictable relationship, a temperature transducer can be composed of the medium itself. If the characteristics of the medium can be defined (e.g., its make up) the transmit time of a sonic pulse through it can be used to determine its temperature. If narrow band ultrasonic transducers are used, they will reject sonic noise that may be occurring in the medium.

A1 periodically generates a short pulse (waveform A, *Figure 4b*) that drives the 2N3440 into conduction, forcing the ultrasonic 40 kHz transducer to emit a short burst at its resonant frequency. The 150V pulse amplitude allows substantial ultrasonic energy to be coupled into the medium. As this pulse is generated, the DM7474 flip-flop is set low (waveform C, *Figure 4b*). After a length of time, determined by the distance between the ultrasonic transducers and the temperature of the gas, the sonic pulse arrives at the receiving transducer and is amplified by A3 and A4 (A4's output is waveform B, *Figure 4b*). This amplified output triggers A6, which resets the flip-flop high. During the time the flip-flop was low, the 2N3810 current source was allowed to charge the 0.01 μ F capacitor (waveform D, *Figure 4b*). When the flip-flop is reset high, Q2 comes on and the charging ceases. The A2 follower output sits at the capacitor's DC potential, which is related to the sonic transit time in the gas stream. The LF398 sample-and-hold is triggered by the "B" DM74121 one shot and samples A2's output. The LF398's output feeds two LH0094 multi-function non-linear converters which are arranged to linearize the speed of sound versus temperature relationship. The output of this configuration is the gas temperature which is displayed on the meter. Gain and zero trims are provided via the A7 and A8 networks. When A1 issues another pulse, the DM74121 "A" one shot resets the 0.01 μ F capacitor to 0V and the entire process repeats.

It is worth noting that no bandwidth limiting of any kind is employed at the A3-A4 receiver despite their compound gain of 1000. This would seem to invite noise sensitivity problems in a sonic system, but the high Q ultrasonic transducer provides almost ideal noise rejection. *Figure 4c* shows the amplified output of the received pulse superimposed on the output of a boardband microphone placed in the sonic path. Boardband noise 100 dB greater than the 40 kHz pulse is pumped into the sonic path. Virtually complete noise rejection occurs and signal integrity is maintained.

PIEZOELECTRIC ACCELEROMETER

Another piezoelectric-based transducer is the piezoelectric accelerometer. These devices utilize the property of certain ceramic materials to produce charge when subject to mechanical excitation. These accelerometers use a mass coupled to the piezoelectric element to generate a force on the element in response to an acceleration's frequency and amplitude. Calibration and sensitivity can be varied by selecting the piezoelectric material and altering the configuration and amount of the mass. The best way to signal condition these devices is to employ an amplifier configuration that is directly sensitive to their charge-type output. Charge amplifiers use low bias current op amps with capacitive feedback. Output voltage will depend upon the charge out of the accelerometer which is related to the applied acceleration.

In *Figure 5a*, the transducer looks directly into the ground potential summing junction of an op amp. Because of this, there is no voltage difference between the interconnecting cable center conductor and its shield. This eliminates cable capacitance effects on the transducer output and allows long cable runs. It is advisable to use cable specified for low triboelectric charge effects for best performance, although this is usually only a factor with relatively low output devices. The $10^{11}\Omega$ resistor provides a DC feedback path, while the variable capacitor sets the sensitivity of the charge-to-voltage conversion. When the accelerometer shown is mounted on a hand-held voltmeter and dropped on the floor, the instantaneous acceleration to which the voltmeter is subjected can be determined. In *Figure 5b*, the stored trace display

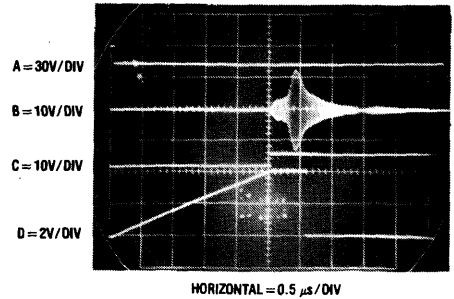


FIGURE 4b

TL/H/5641-6

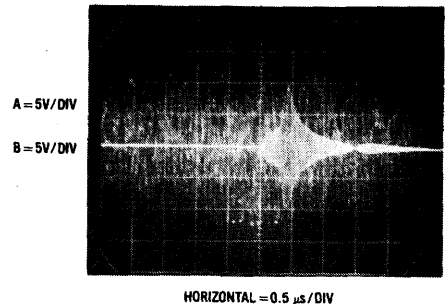


FIGURE 4c

TL/H/5641-7

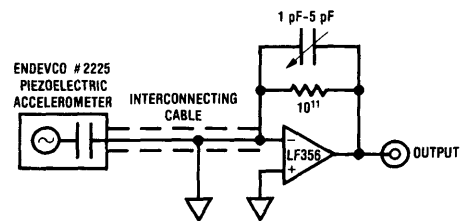
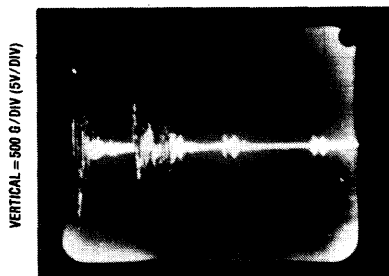


FIGURE 5a

TL/H/5641-8

shows an instantaneous force of almost 1000G with smaller forces generated as the voltmeter bounces 3 times over 60 ms. (It is recommended that this experiment be performed with a borrowed voltmeter.)



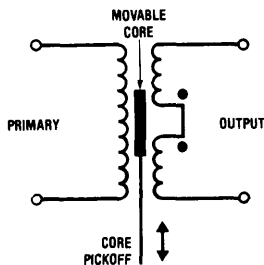
HORIZONTAL = 10 ms / DIV

TL/H/5641-9

FIGURE 5b

LINEAR VARIABLE DIFFERENTIAL TRANSFORMER (LVDT)

The linear variable differential transformer (LVDT) offers zero-friction position sensing with good precision. Although potentiometers are easy to signal condition and allow high precision they cannot match the nearly infinite life and zero-friction of the LVDT approach. LVDTs are available in both rotary and stroke mechanical configurations. The LVDT is basically a transformer (Figure 6a) with a movable core. The primary is driven with a sine wave which is usually amplitude stabilized. The two matched secondaries are connected in series-opposed fashion. When the movable core is positioned in the magnetic (and usually geometric) center of the transformer, the secondaries' outputs cancel and no net secondary voltage appears. This is called the null position. As the core is moved from null, the differential in flux coupled to the two secondaries produces a net voltage difference across them.



TL/H/5641-10

FIGURE 6a

This is the output of transducer. Good transducer performance (e.g., null cancellation characteristics, linearity, etc.) requires manufacturer attention to winding techniques, magnetic shielding, material choices and other issues. Rectifying and filtering the output signal will yield only amplitude information. Optimum signal conditioning requires a phase sensitive demodulation scheme. This gives the amplitude and also polarity information necessary to determine on which side of null the LVDT core is.

Figure 6b shows a circuit which does this. Waveforms of operation are given in Figure 6c. In this circuit, Q1 and its associated components from a phase shift oscillator which runs at 2.5 kHz, the manufacturer's specified transducer operating frequency. A1A amplifies and buffers Q1's output and drives the LVDT (waveform A, Figure 6c). Since the transducer's output will vary with drive level, feedback is used to stabilize the 2.5 kHz amplitude. A1C and A1D full wave rectify a sample of the drive waveform. A1C's filtered output is applied to A1D, a servo amplifier. A1D compares A1C's output to the LM329 reference and drives the Q1 oscillator to complete an amplitude stabilization loop. The LVDT's output is amplified by A2C and fed to A2A. A2A is a unity gain amplifier whose sign alternates between "+" and "-". Synchronous switching for A2A comes from C1 (waveform B, Figure 6c), which is driven by the modulation sine wave output via a phase shift network. The phase trim network compensates phase shift in the LVDT and ensures that C1 switches at the zero crossings relative to A2A's output. When C1's output is low, the 2N4393 FET is off and A2A's positive input (waveform C, Figure 6c) receives signal. When the sine wave reverses polarity, C1's output goes high, turning on the FET, which grounds A2A's "+" input. Under these conditions A2A is always switching its amplification's sign from "+" to "-" in synchronism with the sine wave output from the LVDT. A2A's phase sensitive output, in this case positive, appears in trace D, Figure 6c. A2B provides a scaled and filtered DC output. To trim the circuit, set the LVDT to at least 1/2 physical displacement and adjust the phase trim for maximum output indication. Next, adjust the gain trim for the desired circuit output at full-scale LVDT displacement.

FORCE-BALANCED PENDULOUS ACCELEROMETER

The operating principles of the LVDT are applied in the force-balanced pendulous accelerometer. Transducers of this type feature wide dynamic range, high linearity and very high accuracy. Figure 7a shows one form of a conceptual force-balanced pendulous accelerometer. The device operates by using an LVDT-type pick-off to determine the position of the pendulum. The DC output of the LVDT is fed to a servo amplifier which drives the torque coil. The magnetic output of the torque coil completes a servo loop around the pendulum, forcing it to become immobile. Because the torque coil's field can attract only the pendulum, a second bias coil provides a steady force for the torque coil to work against. When an input acceleration occurs along the sensitive axis, the servo applies the necessary current to the torque coil to keep the pendulum from moving. The amount of current required is directly proportional to the value of the input acceleration. Because the pendulum never moves, transducer linearity and accuracy can be very high. In addition, wide dynamic range is possible. Force-balanced accelerometers are widely applied in aircraft inertial guidance systems, aerospace applications, seismic monitoring, shock and vibration studies, oil drilling platform stabilization and similar applications. In recent years these accelerometers have become available in complete signal conditioned packages, although there are a number of applications where it is desirable to independently signal condition the transducer. Figure 7b shows a detailed schematic of such signal conditioning. The pick-off circuitry is similar to the LVDT shown in Figure 6b and does not require further comment. The bias coil is driven by the LH0002 boosted LF347 (A1A) which is in a current sensing feedback configuration. For the accelerometer shown, the manufacturer specifies

60 mA of bias coil current. Torque pulses are applied by servo amplifier A3B, which is biased from the LVDT demodulator output. The output of the circuit is taken across the 100Ω resistor in series with the torque coil. Servo gain is set at A3B while damping for the loop is provided by the 1 μF unit in A3B's feedback loop. In addition, accelerometer damping is controlled by stabilizing the temperature of the

mechanical assembly. This is accomplished by A3C, which is set up as a simple on-off temperature controller. The interior of the accelerometer is filled at manufacture with a liquid whose viscosity provides appropriate damping characteristics at a specified temperature, in this case 180°F. Accelerometers of this type routinely yield 100ppm accuracy from ranges of 20 mG to 100G.

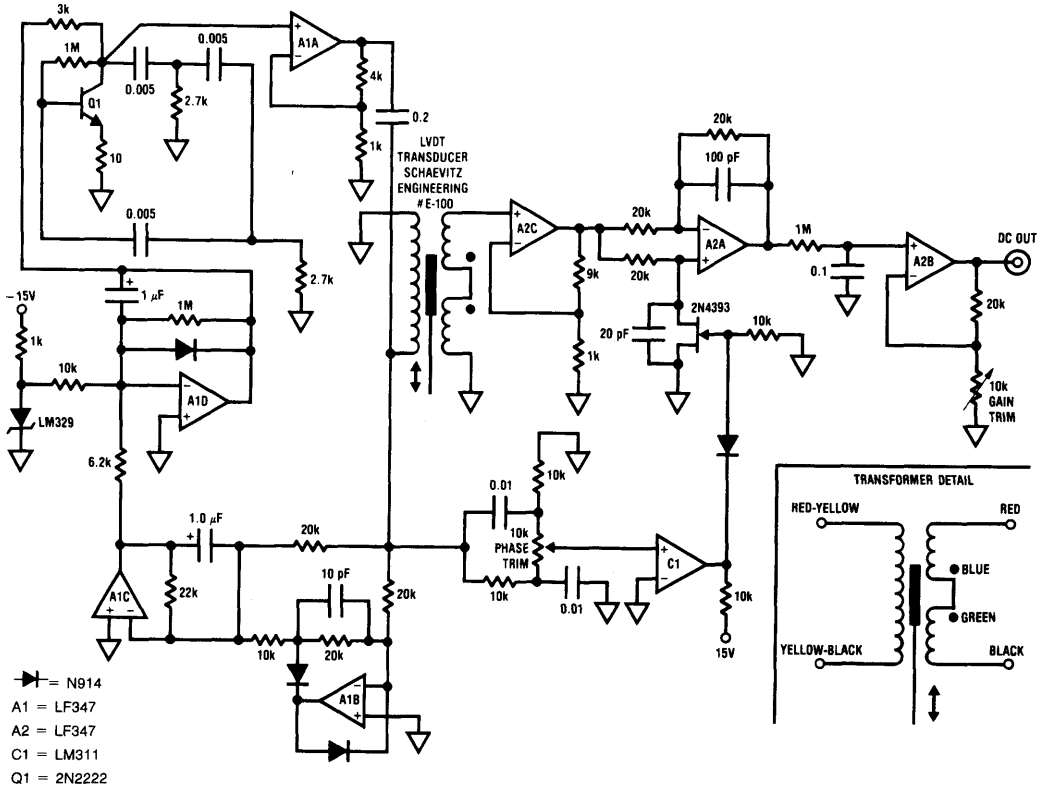


FIGURE 6b

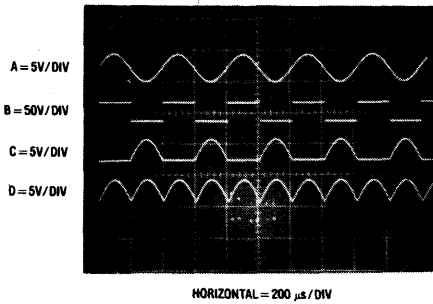


FIGURE 6c

TL/H/5641-12

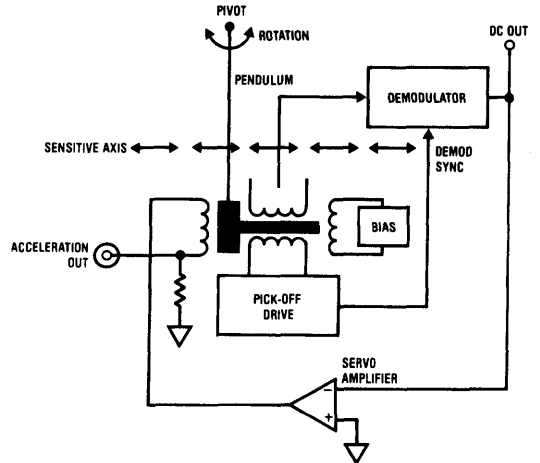


FIGURE 7a

TL/H/5641-11

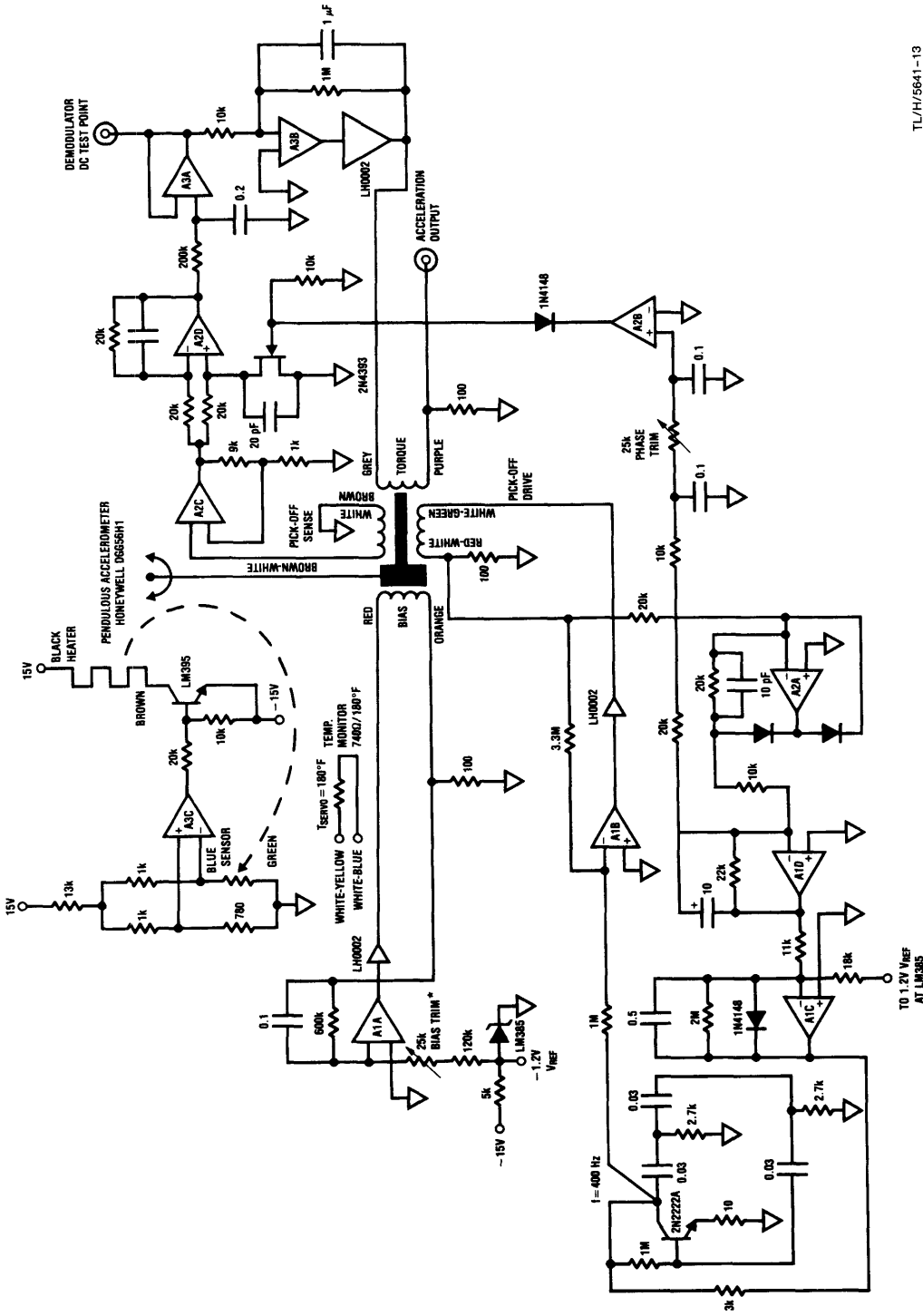


FIGURE 7b

TL/H/5641-13
 *Adjust to 60 mA bias loop current
 A1, A2, A3 = LF347

RATE GYRO

The rate gyro is another form of high performance inertial measuring transducer. It consists of an electrically driven gyroscope with a captive spin axis. Normal gyros are free of restraint and maintain position when moved. The rate gyro is held captive and forced to move with the physical input. By measuring the force generated as the gyro opposes its restraining mechanism, rate-of-angle change information can be deduced. Figure 8 shows signal conditioning for a typical rate gyro. An LVDT-type pick-off is used and synchronous demodulation-type circuitry very similar to Figure 7b is employed. Note the high voltage drive to the gyro motor (26 Vrms) supplied by the boosted LM143. Because of their long life and high precision rate, gyros are frequently employed in inertial guidance systems, drilling platform stabilization systems and other critical applications.

FLUX GATE

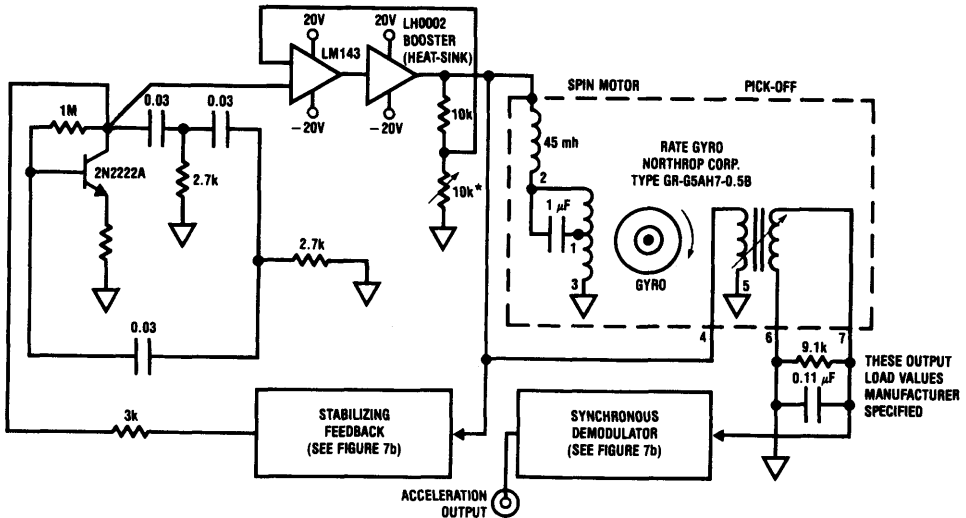
A flux gate transducer converts an external magnetic field (such as that of the earth's) into an electric output. A variety of flux gate configurations exist, the simplest being a piece of easily saturable ferrous material wrapped around a cylinder (Figure 9a). An alternating current is passed along the axis of the cylinder which periodically saturates the material, first clockwise and then counter-clockwise.

A pick-up winding is wrapped around the cylinder. While the ferrous material is between saturation extremes, it maintains a certain average permeability. While in saturation, this permeability ($\mu = dB/dH$) becomes one (an increase in driving field H produces the same increase in flux B). If there is no component of magnetic field along the axis of the cylinder, the flux change seen by the pick-up winding is zero since the excitation flux is normal to the axis of the winding. If, on the other hand, a field component is present along the cylindrical axis, then each time the ferrous material goes from one saturation extreme to the other it produces a pulse output on the signal pick-up winding that is proportional to the

external magnetic field and the average permeability of the material. Since this saturation-to-saturation transition occurs twice each excitation period (fundamental), the frequency of signal out of the pick-up windings is twice the excitation frequency.

These transducers find use in metal detectors, submarine locating gear, electronic compasses, oil surveys, and other areas where measurement of the strength or locally caused disturbance of the earth's magnetic field is of interest. Flux gate transducers are capable of measuring variations in the earth's magnetic field within one gamma (10^{-5} oersteds). Two axis flux gates can be used to construct an electronic compass. More recent flux gate design employs a core-shaped transducer, which is essentially two cylinder types bent together at the ends to form a closed magnetic path. This permits lower driving power and allows the use of commercially available tape-wound cores to be used to construct the transducer. A simple flux gate and its signal conditioning appears in Figure 9b. Excitation to the flux gate is provided by the complementary signal output from the CD4047s. The transistor drives a transformer which is tuned for resonance. This converts the square wave output of the CMOS oscillator into a sinusoidal waveform. This sinusoidal excitation voltage is then converted by the transformer into a high level AC drive current at the excitation frequency which is used to drive the sensor.

The output of the sensor signal winding is an AC signal at twice the excitation frequency and is directly proportional in amplitude to the external axial magnetic field. This second-harmonic of the excitation frequency is then phase detected with a circuit similar to the demodulators shown in Figures 6b and 7b. A portion of the DC output signal may be fed back (shown in dashed lines) to the signal winding to provide a closed loop negative feedback system. This feedback signal produces a field in the sensor which opposes the signal being measured. The high forward gain of the signal channel along with the closed loop negative feedback system ensure good stability and linearity of the output signal.



*Adjust for 26 Vrms output

FIGURE 8

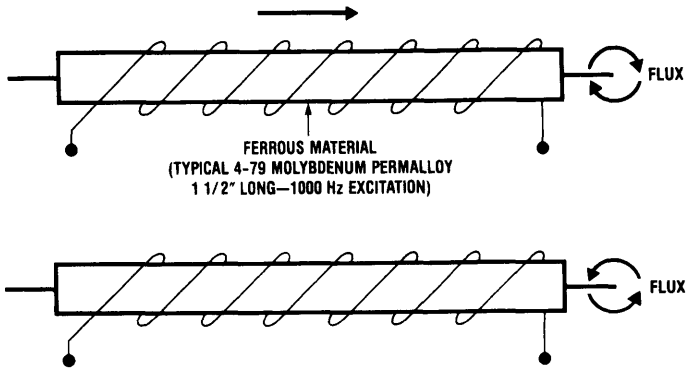


FIGURE 9a

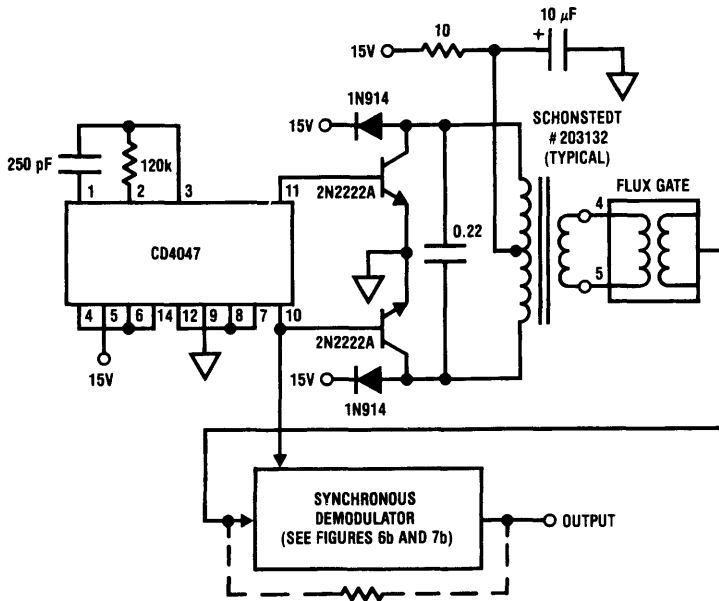


FIGURE 9b

TL/H/5641-15

single-ended output (A2C and A2D) amplifier. A2D's output (waveform C, Figure 10b) feeds the ADC0804 A-D converter. The A-D is triggered by a delayed pulse generated by the A1C and A1D pair (waveform D, Figure 10b). This pulse is positioned so that it occurs after A2D's output has settled to final value. To calibrate the circuit, apply zero physical load to the transducer shown and adjust the zero trim so the A-D converter is just below indicating 1 LSB output. Next, apply (or electrically simulate) 10,000 lbs. and adjust the gain trim for a full output code at the A-D converter.

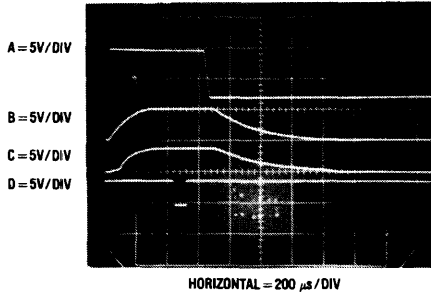


FIGURE 10b

TL/H/5641-17

REFERENCES

- RCA Photomultiplier Handbook*; RCA Electro-Optics Division; Lancaster, PA
- The Pyroelectric Thermometer: A Sensor for Measuring Extremely Small Temperature Changes*; S.B. Lang, McGill University; 1971 International Symposium on Temperature; Washington D.C.
- A User's Guide to Pyroelectric Detection*; Electro-Optical Systems Design; November 1978

Pyroelectric Detectors and Detection Systems; Laser Precision Corp.; Utica, NY

Multiplier Application Guide; Analog Devices Inc.; Norwood, MA; (pages 11-13)

Ultra-Sonic Thermometry using Pulse Techniques; Lynnworth and Carnevale; Panametrics Corporation; Waltham, MA

Handbook of Measurement and Control; Schaevitz Engineering; Pennsauken, NJ

Self-Balancing Flux Gate Magnetometers; William Geyger; AIEE Transactions, Vol. 77, May 1958; Communication and Electronics

A Low Cost Precision Inertial Grade Accelerometer; H.D. Morris; Systron-Donner Corp.; DGON Symposium on Gyro Technology, 1976

Short Form Catalog; ENDEVCO Corporation; San Juan Capistrano, CA

Bulletin 31, MK109 Ultrasonic Transducer; Massa Corporation; Hungham, MA

ACKNOWLEDGEMENTS

The author gratefully acknowledges the cooperation of the following parties who provided transducers, literature and/or advice.

- Hewlett Packard Co., Optoelectronics Division
 Honeywell Inc., Avionics Division
 Laser Precision Corporation
 Schonstedt Instrument Company
 Schaevitz Engineering Company
 Northrop Corporation, Precision Products Division
 RCA Electro-Optics Division
 Lancaster Radiology Associates